



Technical Memorandum No. PMR-TM-66-6

AD 633754

DESCRIPTION AND APPLICATION OF
LASER RADAR AT PACIFIC MISSILE RANGE

By

J. L. KARNEY, et al
Environmental Sciences Division

17 August 1966

PACIFIC MISSILE RANGE

Point Mugu, California

20050218045

CLEARINGHOUSE		
FOR FEDERAL SCIENTIFIC AND		
TECHNICAL INFORMATION		
Library	Microfilm	
1.00	1.50	2.00
/ ARCHIVE COPY		

DDC
RECEIVED
SEP 23 1966
C

DISTRIBUTION OF THIS DOCUMENT IS UNLIMITED.

Best Available Copy

PACIFIC MISSILE RANGE

POINT MUGU, CALIFORNIA

R. N. SHARP, RADM USN

Commander

This report was prepared by Mr. J. L. Karney, Mr. J. E. Masterson, and Mr. W. E. Hochae.

Mr. B. H. Erickson, Acting Head, Environmental Sciences Division; Mr. K. I. Lichti, Acting Deputy Head, Range Operations Department; and Mr. W. L. Miller, Technical Director, Development and Operations, have reviewed this report for publication.

WHITE SECTION <input checked="" type="checkbox"/>
BUFF SECTION <input type="checkbox"/>
<i>For statement on Doc</i>
OR AVAILABILITY CODES
ANAL. OR/OF SPECIAL

Technical Memorandum PMR-TM-66-6

Published by **240910000** Branch
Technical Publications Division
Photo/Graphics Department
First printing 100 copies
Security classification UNCLASSIFIED

Best Available Copy

TABLE OF CONTENTS

	Page
SUMMARY	1
INTRODUCTION	3
DESCRIPTION OF MARK III LIDAR	4
Transmitter and Receiver	4
Method of Operation	7
Method of Data Analysis	8
OBSERVATIONS AND DATA OBTAINED BY LIDAR	9
Clear Air Return	9
Temperature Discontinuities	11
Near-Field Intensity Variations	11
Fog and Low Stratus	12
Multiple Cirrus Cloud Detection	13
Wind Shears	15
Additional Observations	15
FUTURE PLANS	16
CONCLUSIONS	19
TABLE	
Table 1. Characteristics of Mark III LIDAR	7
ILLUSTRATIONS	
Figure 1. Mark III LIDAR System	4
Figure 2. Path Geometry of LIDAR	6
Figure 3. Method of Data Analysis	8
Figure 4. Example of Machine-Reduced Inversion Data	10
Figure 5. LIDAR Returns from Clear Atmosphere	10
Figure 6. LIDAR Detection of Inversion Layer	11
Figure 7. Traces from Before and After Sunrise Showing Change in Near-Field Backscatter Intensity	12
Figure 8. Example of LIDAR Penetration of Stratus Layer	13
Figure 9. LIDAR Detection of Cirrus Through Stratus Overcast	14
Figure 10. Example of Multiple Cirrus Cloud Detection	14
Figure 11. Example of Possible Wind Shear Detection	15
Figure 12. Effect of Solar Radiation on LIDAR Return as a Function of Azimuth Angle	16
Figure 13. Solar Effects on LIDAR Return Before and After Sunset	17
Figure 14. Solar Effects on LIDAR Return Before and After Sunrise	18

SUMMARY

A cooperative effort was undertaken by the Office of Naval Research, the Pacific Missile Range, and the Naval Air Systems Command to implement a proposed Stanford Research Institute program to design and fabricate a small laser radar to serve as a quasi-operational device for meteorological research. This prototype device, called the Mark III LIDAR (Light Detection and Ranging) was delivered to the Pacific Missile Range in February 1965 and is presently undergoing operational evaluation. A preliminary description of the data and results obtained are given.

The LIDAR is a new and unique tool which promises to provide meteorologists and atmospheric physicists a means to accomplish tasks not possible using present equipment. The LIDAR may someday assist the meteorologist in making short-range forecasts by providing slant-range visibility data and quantitative measurements of stratus density and fog thickness.

The LIDAR is capable of determining precise ranges to clouds (together with their bases and tops), measuring the height of temperature inversions, and detecting atmospheric phenomena in apparently clear atmospheres. At the present time, the LIDAR data are used in conjunction with observations from other sources to supplement and improve existing weather information. With relatively minor modifications, the LIDAR could significantly augment the present methods of gathering atmospheric data.

INTRODUCTION

An indirect means of measuring atmospheric variables has been sought by meteorologists and atmospheric physicists for many years. Radar has been used extensively and with considerable success especially in tracking storms and rain clouds, and measuring precipitation processes. The indirect method is an inexpensive and desirable way of obtaining on-site data whereby the instrumentation remains on the ground and balloon or rocket vehicles and equipment are not expended.

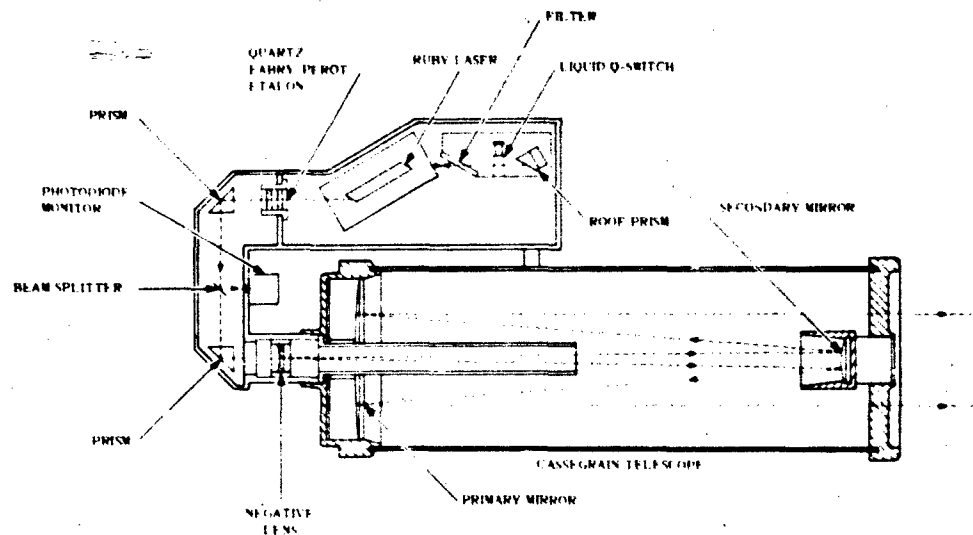
Hulbert and Elterman, in their early attempts at measuring atmospheric density by searchlight techniques, pioneered in the use of the light beam as an indirect measuring tool. Just after Maiman fabricated the first laser in 1960, Goyer, * Ligda, * Shotland, Atlas, and others quickly recognized that the laser could be a new tool for the meteorologist rather than just a scientific curiosity. Among the first to employ the laser in meteorological research were Ligda and his associates at the Stanford Research Institute (SRI). Since 1963, the research workers at SRI have demonstrated the feasibility of using pulsed ruby lasers for cloud detection and ranging, measurements of inversion height, and detection of discontinuities in clear air, to cite a few examples. SRI proposed to the Office of Naval Research that they fabricate a much larger and more powerful laser radar and carry out scientific research into its uses as a tool for making atmospheric measurements. Because the Pacific Missile Range has continuing requirements for atmospheric measurements, a cooperative effort was undertaken by the Office of Naval Research, the Pacific Missile Range, and the Naval Air Systems Command to implement the proposed SRI program. This program provided the design and fabrication of a small laser radar to serve as a quasi-operational device. This prototype device, called the Mark III LIDAR (Light Detection and Ranging), was delivered to the Pacific Missile Range in February 1965, and it is presently undergoing operational evaluation. During this evaluation, significant data and operationally useful results have been obtained. A description of the Mark III LIDAR and a brief account of the results obtained are presented herein.

*See G. G. Goyer and R. Watson. "The Laser and its Application to Meteorology," Bulletin of the American Meteorological Society. Vol. 44, No. 9, pp. 564-570. See also M. G. E. Ligda. "Meteorological Observations With LIDAR," presented at Office of Naval Research First Conference on Laser Technology. Boston, Mass., 12-14 Nov 1963. SECRET.

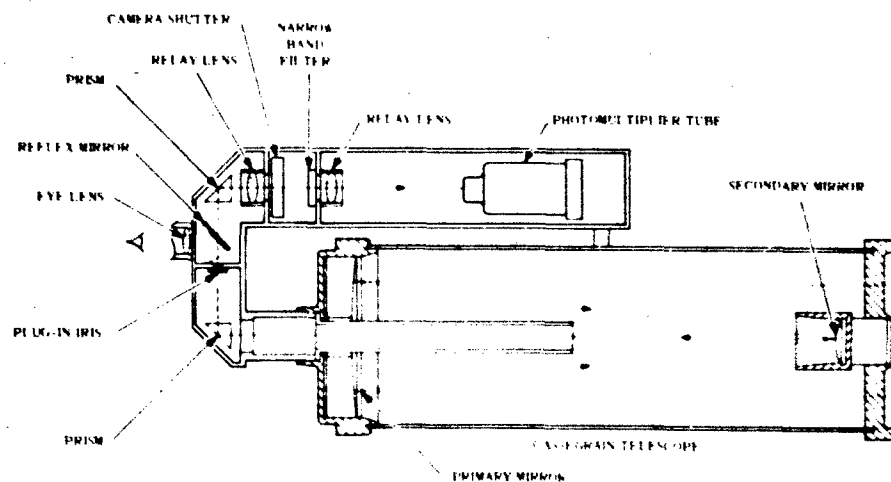
DESCRIPTION OF MARK III LIDAR

Transmitter and Receiver

The transmitter of the Mark III LIDAR system, as shown in figure 1(a), consists of a ruby laser and the optical components necessary for directing the laser beam into an 8-inch Cassegrainian telescope. Lasing action is accomplished by energizing, with approximately 1,600 joules of energy, two linear flash tubes fired in series. By means of a Q-switch, a single pulse, 20 to 30 nanoseconds in duration and with 5 to 40 megawatts of power, is generated. The Q-switch is an absorbing dye solution (vanadium phthalocyanine) that does not require a separate power supply or electronic triggering for activation. Proper manipulation of the dye concentrations in the Q-switch will change the output power level resulting in a shorter pulse but having a greater peak amplitude.

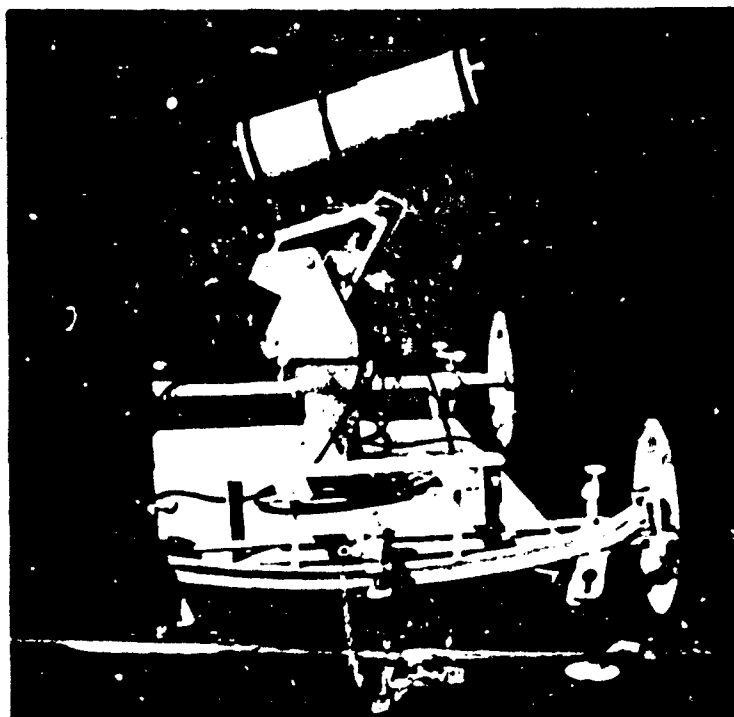


(a). Transmitter.

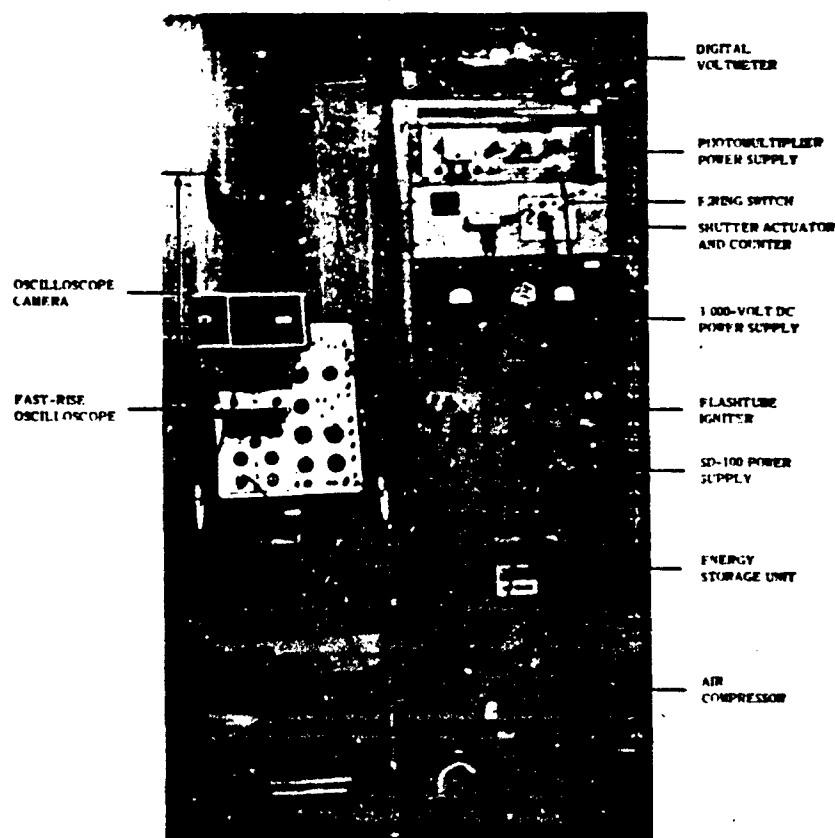


(b). Receiver.

Figure 1. Mark III LIDAR System.



(c). LIDAR on Transportable Mounting.



(d). Rack Equipment and Power Supplies for LIDAR.

Figure 1. (Concluded).

Calibration and monitoring of the laser output energy is accomplished by recording the output pulse energy from a fast-response photodiode located in the transmitter. The single pulse generated by the photodiode is also used for initiation of a sweep circuit in the output oscilloscope.

The receiver of the LIDAR system (see figure 1(b)) consists of a high-gain, low-noise photomultiplier tube mounted at the focus of an 8-inch Cassegranian telescope. The transmitter and receiver are mounted parallel with 3 inches separation between the telescope assemblies. A parallax adjustment is used to vary the region of intersection of the transmitted beam and receiver field of view (see figure 2). A set of field stops can be used in the receiver to limit the field of view and enhance the signal-to-noise ratio. A 10-angstrom interference filter with pass band centered at 6943 angstroms, is used for daytime observations to reduce the background level (noise) to an intensity significantly below that of the backscattered signal. Near-field alignment of the receiver optics with the backscattered return is easily accomplished by manually sighting through the receiver telescope and performing the necessary adjustment. A summary of the LIDAR transmitter and receiver characteristics appears in table 1.

The LIDAR and associated electronics are designed for portable installation and require only nominal external power. Following equipment setup, the time required to obtain and process one observation is under 5 minutes. Because of the simplicity of the instrument and the operating procedure, only one technician is needed to operate the LIDAR. Safety considerations, however, require two personnel to be present.

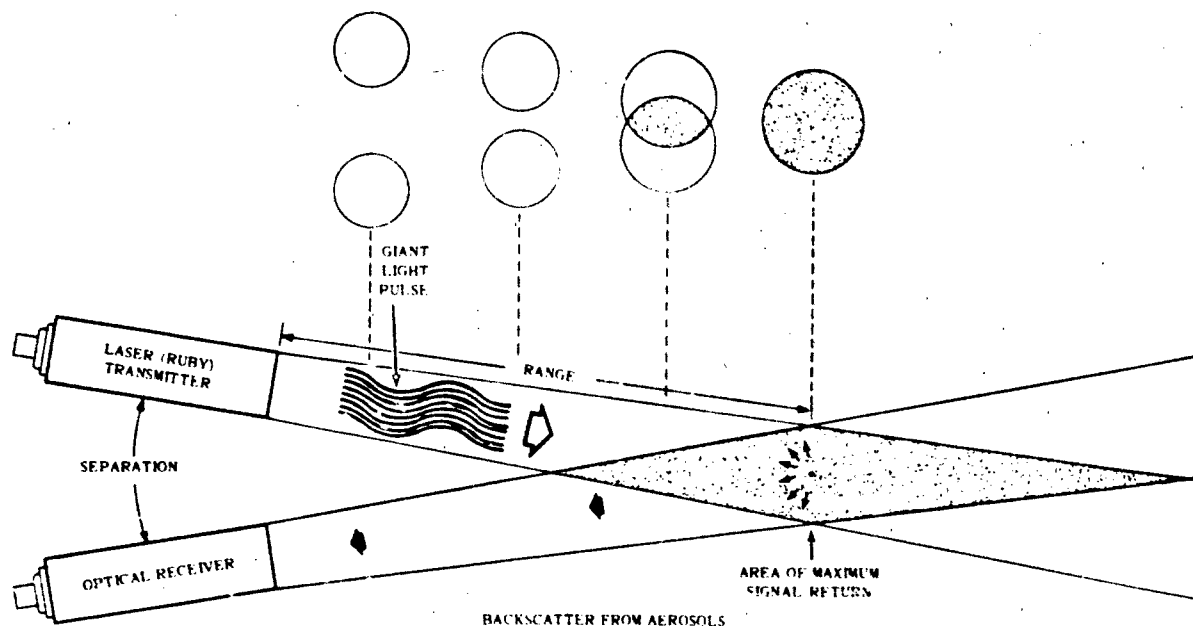


Figure 2. Path Geometry of LIDAR.

Table 1. Characteristics of Mark III LIDAR

Transmitter

Laser: One ruby crystal, approximately 3 inches long by $\frac{1}{2}$ -inch diameter, with Brewster angles on each end. Output wavelength is 6943 angstroms.

Power supply: 0 to 5 kilovolts, 150 milliamperes max. red.

Q-switch: Saturable-filter; vanadium phthalocyanine in solution with CHCl_3 .

Beamwidth: Output from 8-inch Cassegranian telescope. Beam area 50.24 square inches.

Pulse Length: 20 to 30 nanoseconds.

Transmitted energy: 0.3 joule.

Transmitted power: Normal operation of 5 megawatts per pulse. Peak power of 40 megawatts.

Beam divergence: 0.5 milliradian.

Flash tubes: Two xenon flash tubes energized by 2,500 to 2,700 volts.

Temperature control: Forced air or gas cooling.

Pulse rate frequency: Once every 3 minutes.

Receiver

Beamwidth: Adjustable with iris in focal plane of an 8-inch Cassegranian telescope. Nominal field of view is 0.8 milliradian.

Detectors: International Telephone and Telegraph FW-130 photomultiplier tube with S-20 response. Quantum efficiency approximately 3 per cent for wavelength of interest. Counting rate when tube is in dark state is approximately 100 pulses per second.

Bandpass: Maximum 11 angstroms (adjustable).

Data output: Oscilloscope presentation from output of photomultiplier.

Method of Operation

The path geometry of the LIDAR and the technique of recording the scattered light pulses are shown in figure 2. A pulse of light leaving the transmitter is scattered from aerosols or cloud particles in the atmosphere. The fraction of the light energy backscattered from the atmosphere and passing through the 8-inch aperture of the receiver telescope constitutes the LIDAR signal. After passing through the 10-angstrom filter, the signal is incident on a high-gain, low-noise, photomultiplier tube. The resulting analog voltage from the photomultiplier tube is then displayed on a wide-band oscilloscope where the instantaneous display is photographed by a Polaroid camera using a special high-speed film.

Method of Data Analysis

The technique of interpreting the recorded data is illustrated in figure 3. This generalized example shows the LIDAR and the information returned from a typical return. The display is similar to a profile of the atmosphere with the abscissa as time (or range) and the ordinate as the relative intensity of the backscatter from the aerosol or cloud target. The backscattered light from an atmospheric target appears as a vertical deflection of the trace similar to a radar A-scope presentation. The time between transmission of the pulse and the arrival of the signal can be correlated to distance and used to compute altitude if the elevation angle is known. When the elevation angle is accurately measured, the LIDAR is capable of measuring distances and altitudes to targets with accuracies of several feet.

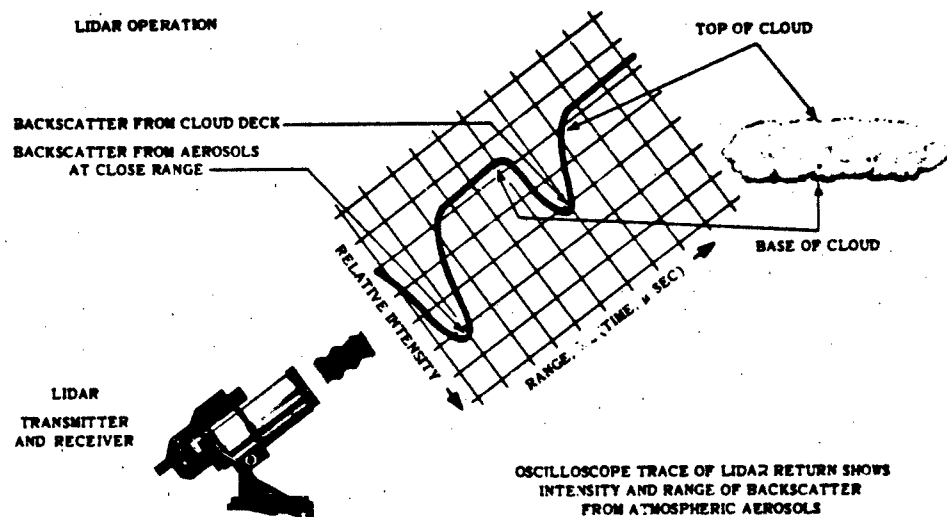


Figure 3. Method of Data Analysis.

When the target is a stratus or cirrus cloud for example, the echo is similar to the second spike in figure 3. The base and top of the cloud are represented by the front and back portions of the spike. The signal intensity is proportional to the size and composition of the scattering particles, their relative density or population within the cloud, and their distance from the receiver. Intensity variations within the echoes from cloud targets indicate inner structure or density variations. Signal intensity from the target is recorded along with the normal background intensity of the sky light (sky brightness). Should the laser pulse penetrate through a cloud, the signal then returned to the photomultiplier tube approaches the background intensity due to attenuation of the backscatter by the intervening cloud layer.

In figure 3, the large spike at close range, or in the foreground, represents backscatter from the aerosols in the lower atmosphere immediately in front of the LIDAR. This "near-field" scattering extends to approximately 5,000 yards distance from the transmitter. Scattering of the laser pulse from atmospheric

particles of dimension equal to or greater than 0.7 micron, or Mie scattering, predominates over molecular or Rayleigh scattering. The data accumulated indicates that the magnitude of this near-field return depends largely upon the concentration and size distribution of aerosols, the divergence of the transmitter and receiver optical axes, and the particular elevation angle of the LIDAR. On many occasions, observations have shown that the peak intensity of this near-field return fluctuates over several hours. These fluctuations appear to correspond to changes in visibility, although actual correlations have not been tested.

Although most of the LIDAR measurements have been made between elevation angles of 20 to 60 degrees, returns at 90 degrees can be obtained. However, when the instrument is pointing vertically the data from the lower atmosphere displayed on the oscilloscope and recorded on Polaroid film, is too compressed for good altitude resolution.

Interpreting the signal information directly from the Polaroid prints can sometimes be misleading because of the normal inverse square law decrease of the backscattered light with range. A method for reducing the Polaroid data has been devised which involves plotting the logarithm of the intensity against the logarithm of the slant range. This is illustrated in figure 4. When plotted, the normal intensity falloff will appear as a straight line. Any signal variations resulting from discontinuities in the atmosphere will appear as variations in line slope.

This data-reduction method has now been accomplished by machine methods whereby each Polaroid data trace is divided into increments of time and intensity, manually digitized on cards, and tabulated for either automatic or manual plotting.

OBSERVATIONS AND DATA OBTAINED BY LIDAR

Clear Air Return

The scattering of light radiation is an inherent property in any particulate atmosphere. In the Point Mugu area, situated on the Pacific coast, light scattering will result primarily from particles larger than the wavelength of light. This is usually termed Mie scattering. These large particles, approximately 0.1 to 5.0 microns in diameter, are composed of water droplets, salt spray, and sand or dust, and are invisible to the eye. LIDAR returns from an otherwise clear atmosphere sometimes reveal a fine aerosol structure arrayed in layers which extend to altitudes of several thousand feet. This layered structure has also been found to exist during mild winds when a thorough mixing of the lower atmosphere is assumed. An example of a clear air return exhibiting a complicated aerosol structure is shown in figure 5 together with an interpretation of the aerosol density distribution. Although a 2.0- to 5.0-knot wind existed at ground level, this particular aerosol structure persisted for several hours. The temperature profile for that day, also plotted, shows a significant

temperature inversion. Aerosol density variations of this type, in which the number, optical density, and sizes of the particles vary, are difficult to interpret in terms of total scattering and scattering cross section.

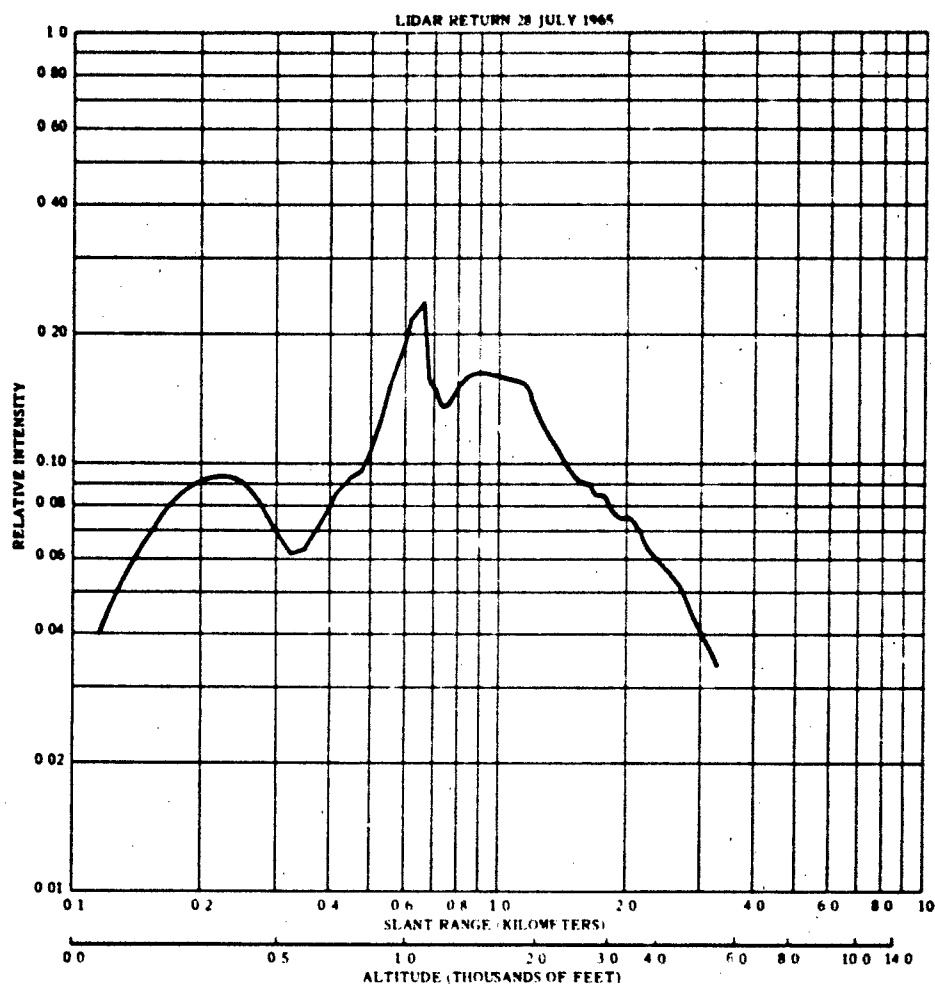


Figure 4. Example of Machine-Reduced Inversion Data.

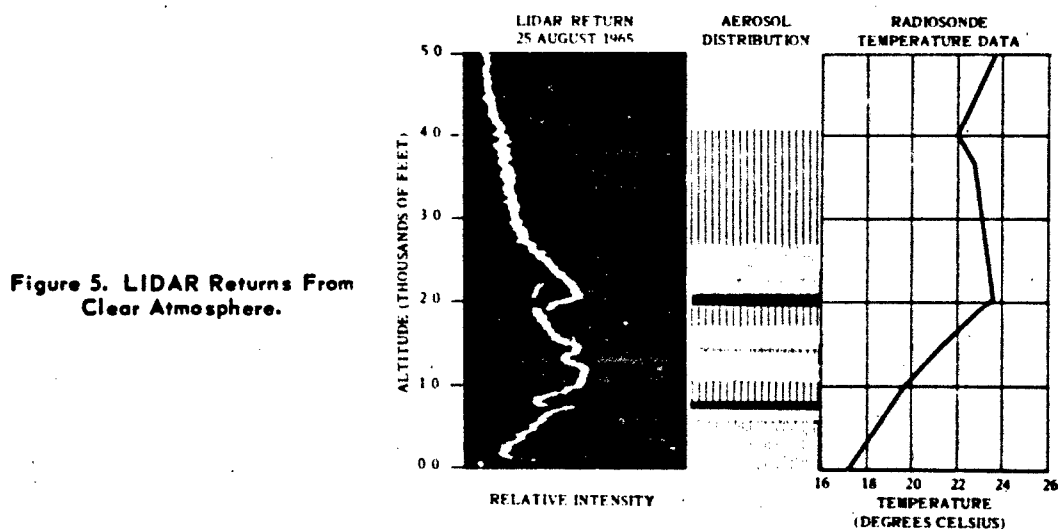


Figure 5. LIDAR Returns From Clear Atmosphere.

Temperature Discontinuities

Because of the tendency of aerosols to concentrate in layers in the stable air just above the temperature inversion base, a backscatter is obtained from this region and it appears as an echo in the LIDAR return. Even in clear air conditions, the height and short-term variability of height of coastal temperature inversions can be measured. At this time the LIDAR is capable of detecting only the presence of these inversions and not their magnitude, i.e., the temperature gradient.

A good example of inversion occurrence detected by the LIDAR in a clear atmosphere is shown in figure 6, together with the radiosonde record for the same day. The LIDAR trace shows a definite echo at 1,000 feet altitude, resulting from a thin aerosol layer at the inversion base. The slope of backscattered intensity appears normal up to 2,100 feet where the slope changes apart from the usual intensity falloff. This corresponds to the light pulse leaving the region of stratified air and entering cleaner air above the inversion top. An example of inversion data reduced by machine methods appears in figure 4.

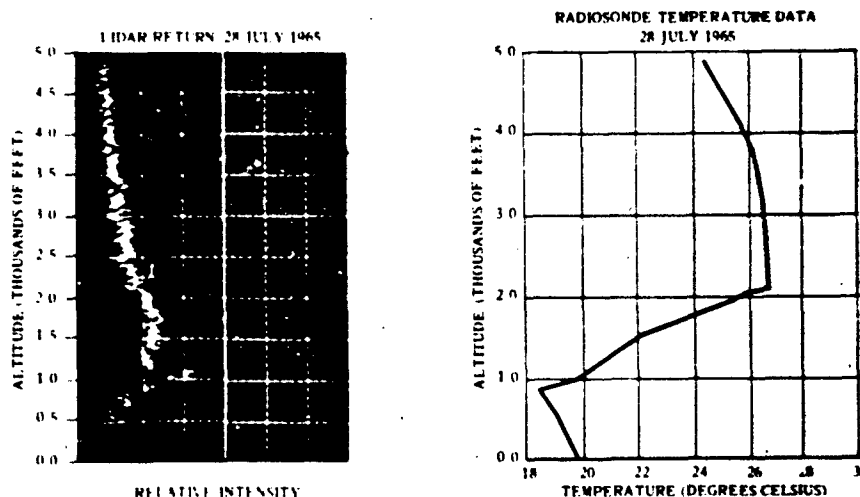


Figure 6. LIDAR Detection of Inversion Layer.

Near-Field Intensity Variations

It has been determined, from a large number of atmospheric returns, that the amplitude of the near-field portion of the trace for a given elevation angle is a function of atmospheric conditions close to the LIDAR (from 100 to 500 yards range). The characteristics of the scattering medium in this range can change throughout the day, from inclusions of fog, haze, dust, or pollutants. A series of LIDAR observations obtained over a period of minutes to several hours may show variations in signal intensity arising from changes in the "near-field" region of the atmosphere. These changes in backscatter return are proportional to the visibility changes that also occur.

A similar change in near-field backscatter intensity is apparent when comparing laser returns taken before and after sunrise or sunset. As shown in figure 7, different characteristics and stronger signal amplitudes are evident in the near-field return after sunset. This effect may be partially attributed to an increase in size of hygroscopic nuclei by collecting water molecules. An increase in the near-field scattering could also result from precipitation of larger nuclei (0.1 micron to 1.0 micron) from the higher altitudes in the absence of thermal turbulence and eddies after sunset.

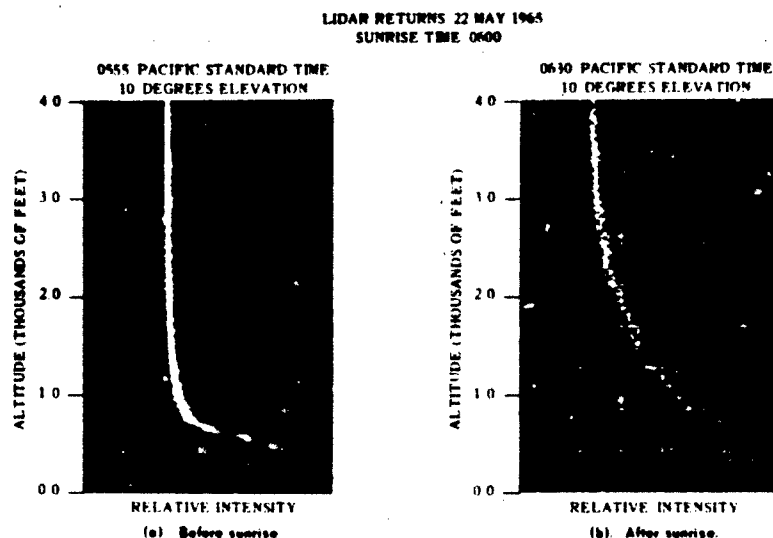


Figure 7. Traces From Before and After Sunrise Showing Change in Near-Field Backscatter Intensity.

Fog and Low Stratus

One of the primary applications of the LIDAR is to measure the height and thickness of coastal stratus. A typical LIDAR echo from stratus contains information on heights of the top and base and the relative density of the stratus. To measure the depth of a fog or stratus layer, it was necessary to determine if the laser pulse was penetrating through the top of the layer. Observations were made at several elevation angles to obtain criteria for discrimination between gradual extinction of the laser pulse by the fog and the penetration of the top of the stratus layer. Figure 8 shows LIDAR returns obtained for a typical stratus or fog condition. The gradual decrease in signal intensity in figure 8(a) is due to extinction of the laser pulse in contrast to the sharp cutoff shown in figure 8(b) and figure 8(c).

The signal amplitude in figure 8(b) is shown to increase to a maximum limit and then sharply decrease to an extremely low noise level for the continuation of the trace. These changes in scattering intensity are a result of the laser pulse penetrating the dense region of fog particles and entering the clear air above the relative flat stratus top. Scattering of the laser pulse from this region is not detected because of the stratus attenuation of these weaker signals from the clear air.

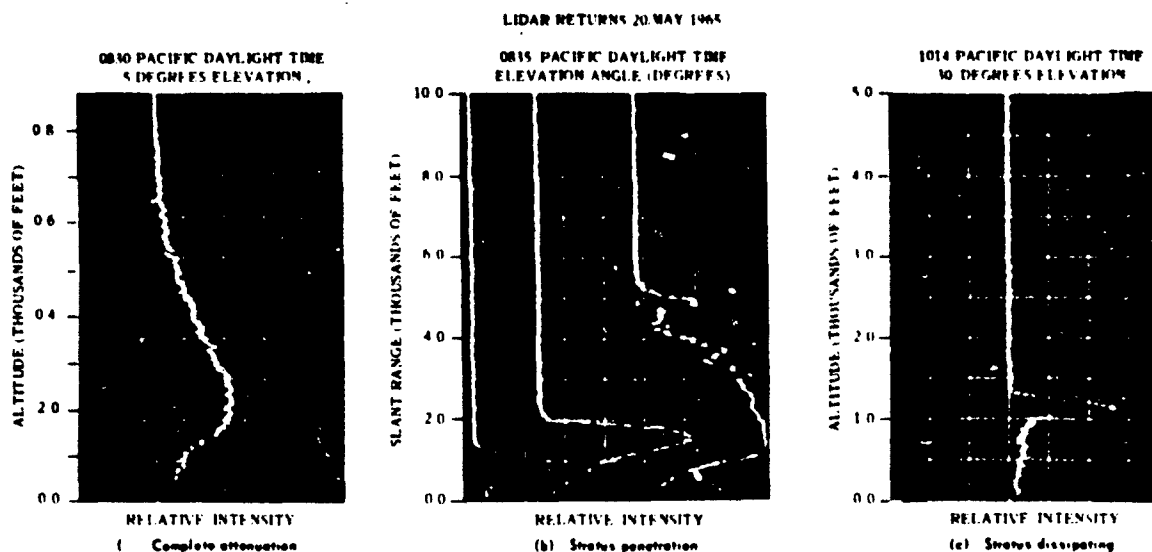


Figure 8. Example of LIDAR Penetration of Stratus Layer.

With a knowledge of the elevation angle, these observations place the top of the stratus at approximately 1,000 feet. Correlation with actual meteorological conditions was accomplished by using radiosondes, ceilometers, ground observers, and aircraft reports. LIDAR returns, obtained later that morning, figure 8(c), indicated the stratus base had lifted slightly and was in the process of dissipation. Complete dissipation did not occur until midday.

The LIDAR capability to penetrate through a stratus overcast and to detect and measure the thickness of higher clouds has been demonstrated at Point Mugu. During operations on 5 April 1965, a high cloud layer was detected above a lower stratus overcast, as shown in figure 9. The echo from the stratus layer in figure 9(a) was at approximately 6,000 feet altitude during the morning but the overcast did not dissipate until late afternoon. The stratus overcast was 300 feet thick. LIDAR echoes received through the overcast indicated the presence of low cirrus in one layer extending from 21,000 to 26,000 feet altitude. In figure 9(b), the return from 70 degrees elevation shows the existence of the stratus and the cirrus layers obtained with one measurement. Although this higher cloud layer was detected by the LIDAR at 1020 hours, it was not reported by the meteorological observer until later in the afternoon due to low stratus overcast. Observation during any overcast condition necessitates the use of neutral density filters to reduce the level of backscatter intensity to the photomultiplier tube. The over-all signal magnitude of returns shown in figure 9 have been reduced by 50 per cent to prevent photomultiplier saturation.

Multiple Cirrus Cloud Detection

An example of multiple cirrus cloud detection together with a water vapor profile for correlation is shown in figure 10. The echoes in the LIDAR return in figure 10(b) were obtained from cumulus at 3,300 feet, altostratus at 14,300 feet, and multiple cirrus cloud layers at 22,200 feet and 24,700 feet altitude.

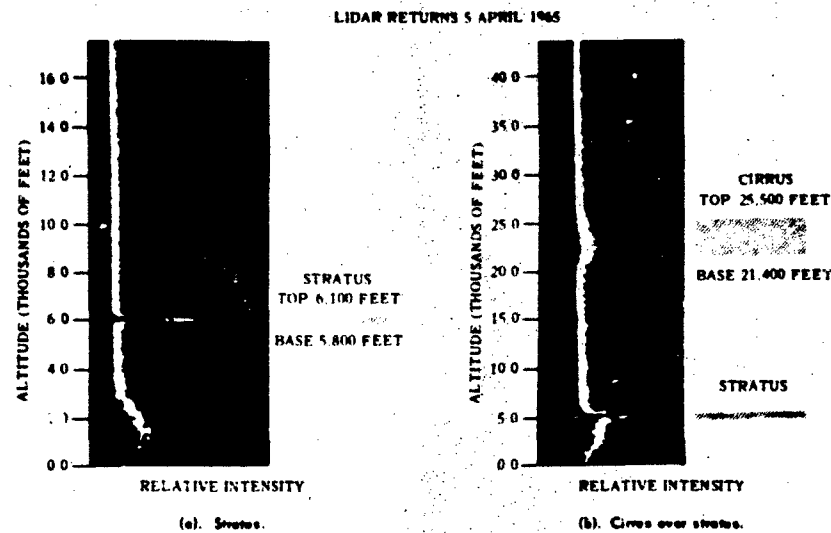


Figure 9. LIDAR Detection of Cirrus Through Stratus Overcast.

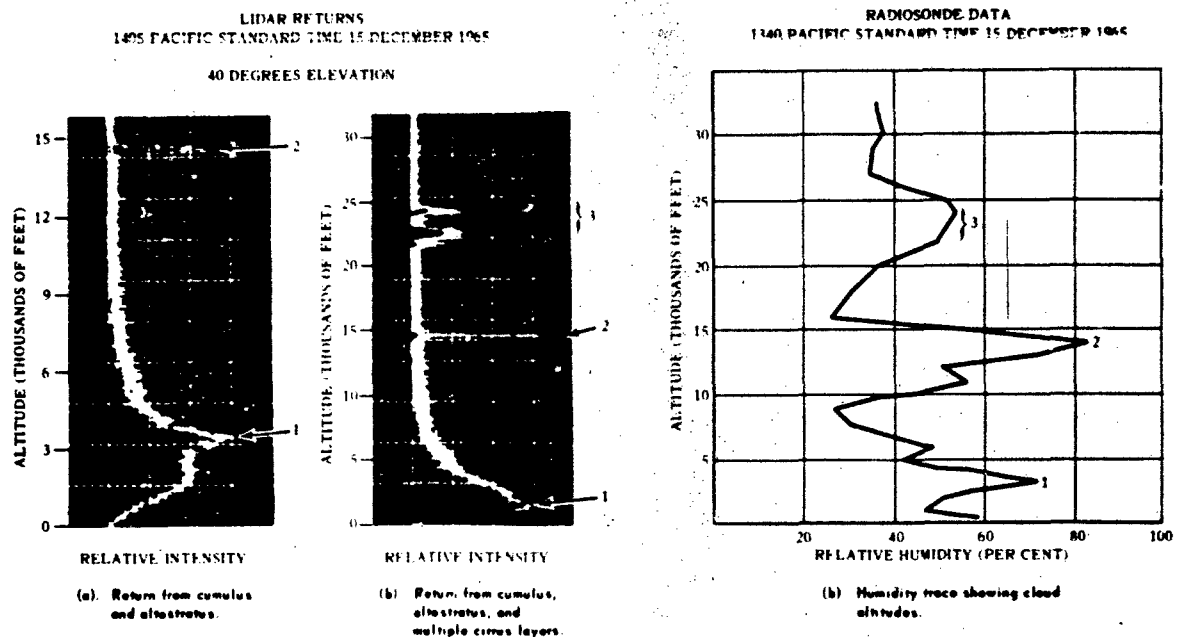


Figure 10. Example of Multiple Cirrus Cloud Detection.

Figure 10(a) is the LIDAR return from the lower atmosphere showing in detail the cumulus and altostratus cloud layers. The cirrus was visible from the ground above scattered to broken cumulus but it could not be discerned if multiple layers existed. A humidity profile obtained from a radiosonde will show relative maximum values in the vicinity of clouds or areas of high water vapor content. The humidity profile for that day, figure 10(c), agrees with the cloud altitudes provided by the LIDAR. This method gives information on the exact height of cirrus, the thickness of cirrus layers, and the distribution of multiple cloud layers which are not available from observations by ground observers, and are often difficult to interpret from radiosonde data.

Vind Shears

Observations over a period of time indicated that LIDAR echoes may be obtained from phenomena associated with wind shears in the upper atmosphere. On one occasion, unusual echoes were received by the LIDAR from an altitude of 66,000 feet in an otherwise clear atmosphere. These echoes persisted for about 30 minutes. An effort was made to correlate these returns with available meteorological information. Results from an observation on 15 April, together with local wind data taken from a radiosonde are shown in figure 11. As indicated by the hodograph, figure 11(b), a moderate wind shear existed in the region where the LIDAR echo originated. It is believed that a signal of this magnitude could not have originated by reflection from the boundary layer separating the turbulent region. These signals were probably generated by scattering from stratospheric dust or ice crystals trapped in the discontinuity of the turbulent layers.

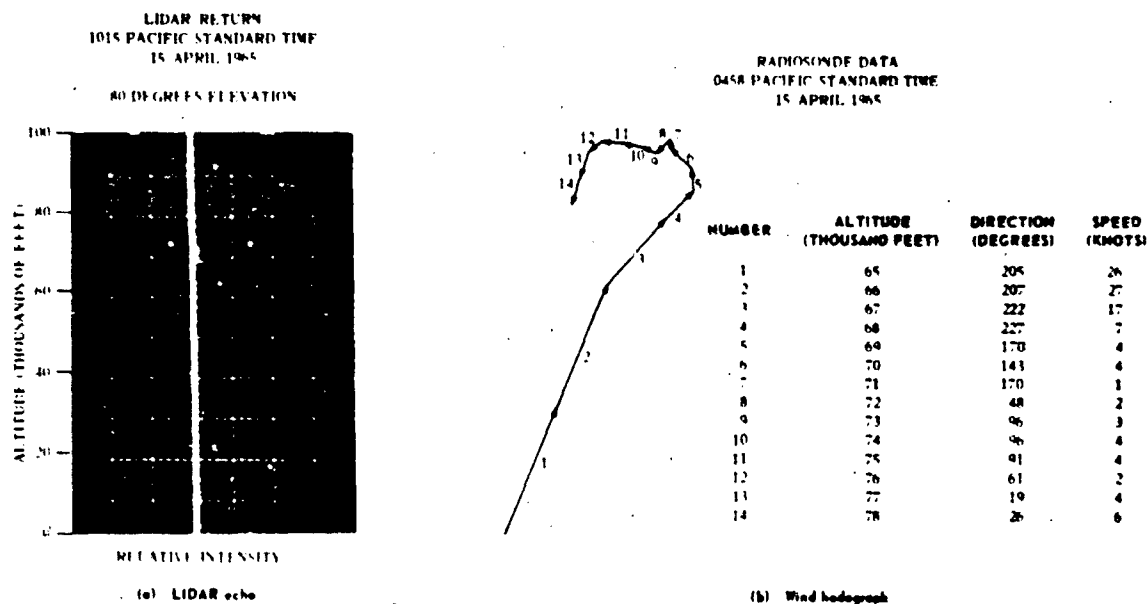


Figure 11. Example of Possible Wind Shear Detection.

Additional Observations

During certain early morning observations, differences in the over-all amplitude of returns or intensity of backscatter were noted which could not be attributed to changes in the density of scatterers present but was connected with solar radiation or solar elevation angle. Occurrences of this particular phenomenon were restricted to the hours of sunrise and sunset. Typical LIDAR returns of this phenomena are shown in figure 12. During the time when the solar elevation angle was between 10 and 20 degrees above the horizon, a considerable decrease in signal amplitude was noted for observations at particular azimuth angles. A minimum signal amplitude occurs when the LIDAR is perpendicular to the sun's plane of motion upon comparing observations in the solar or antisolar direction.

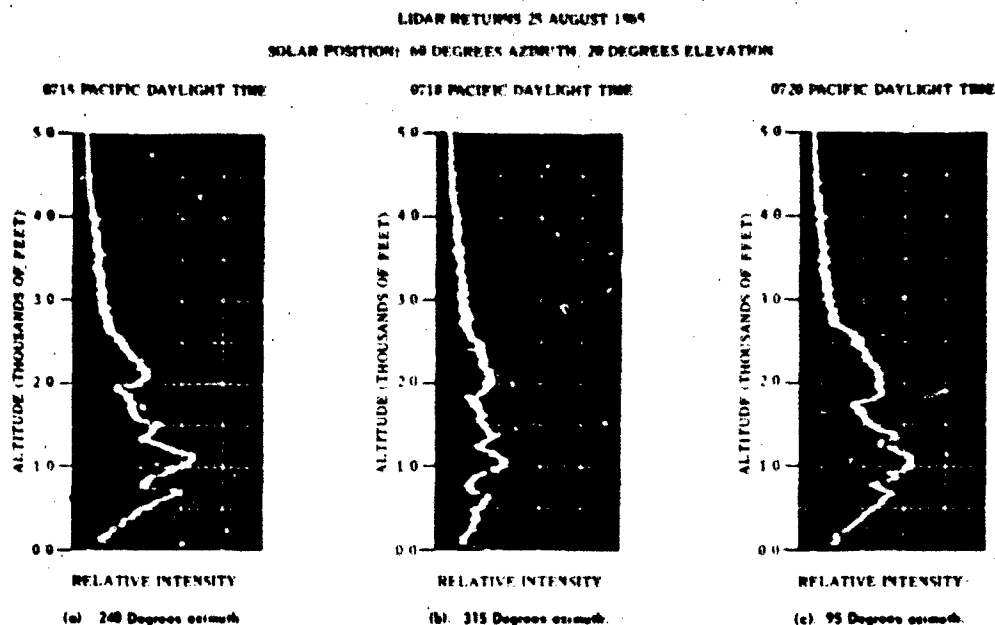


Figure 12. Effect of Solar Radiation on LIDAR Return
as a Function of Azimuth Angle.

LIDAR results obtained on 4 May and 22 May, which are shown reduced and plotted in figures 13 and 14, respectively, are typical. In figure 13, the returns from before and after sunset from three different azimuth angles are plotted simultaneously. There is an over-all decrease in magnitude occurring after sunset at which time the returns from any azimuth direction are usually identical. This condition as represented in figure 13 by trace numbers 1, 2, and 3 is typical of homogeneously scattering atmosphere. However, trace number 4 shows a distinct intensity shift before sunset for one direction (south) at approximately 90 degrees from the setting sun. This shift is also present for north azimuth angles. When the same procedure was applied to LIDAR returns before and after sunrise, similar results appeared. The after-sunrise results of 22 May show a pronounced shift in signal intensity for the north-south direction indicating almost no signal return.

Although background intensity (sky illuminance) and sky polarization effects were analyzed, no evidence would be found to permit the results to be interpreted in terms of known atmospheric anomalies. It is possible that the effect of beam polarization on the atmospheric scatterers is responsible for the effects observed. One interpretation of this situation is that the capabilities of the LIDAR are not being fully exploited.

FUTURE PLANS

The findings presented at this time represent only a small fraction of the capability of the laser radar for meteorological observations. When this capability is realized, perhaps more investigators will enter the field to verify and add their findings to the results already obtained. Observations of the solar dependence on laser backscatter and the near-field variations before and after

rise and sunset will continue, but effort will also be directed toward other meaningful returns from the "clear atmosphere." The results should yield valuable information to workers in the fields of laser communication, weapons detection, and meteorology.

Preliminary results of analyzing LIDAR echoes from various targets such as buildings, ground cover, and clouds, indicate more analysis is required. Further analysis and possibly phase and polarization measurements may yield more information on the identity and characteristics of targets. The polarization of backscattered light will be investigated as a means of identifying cloud compositions (i.e., ice crystals or water vapor.)

The LIDAR is in a favorable position at Point Mugu to study the effects that a large body of water has on transmission. The results can be examined for significance using presently available capabilities.

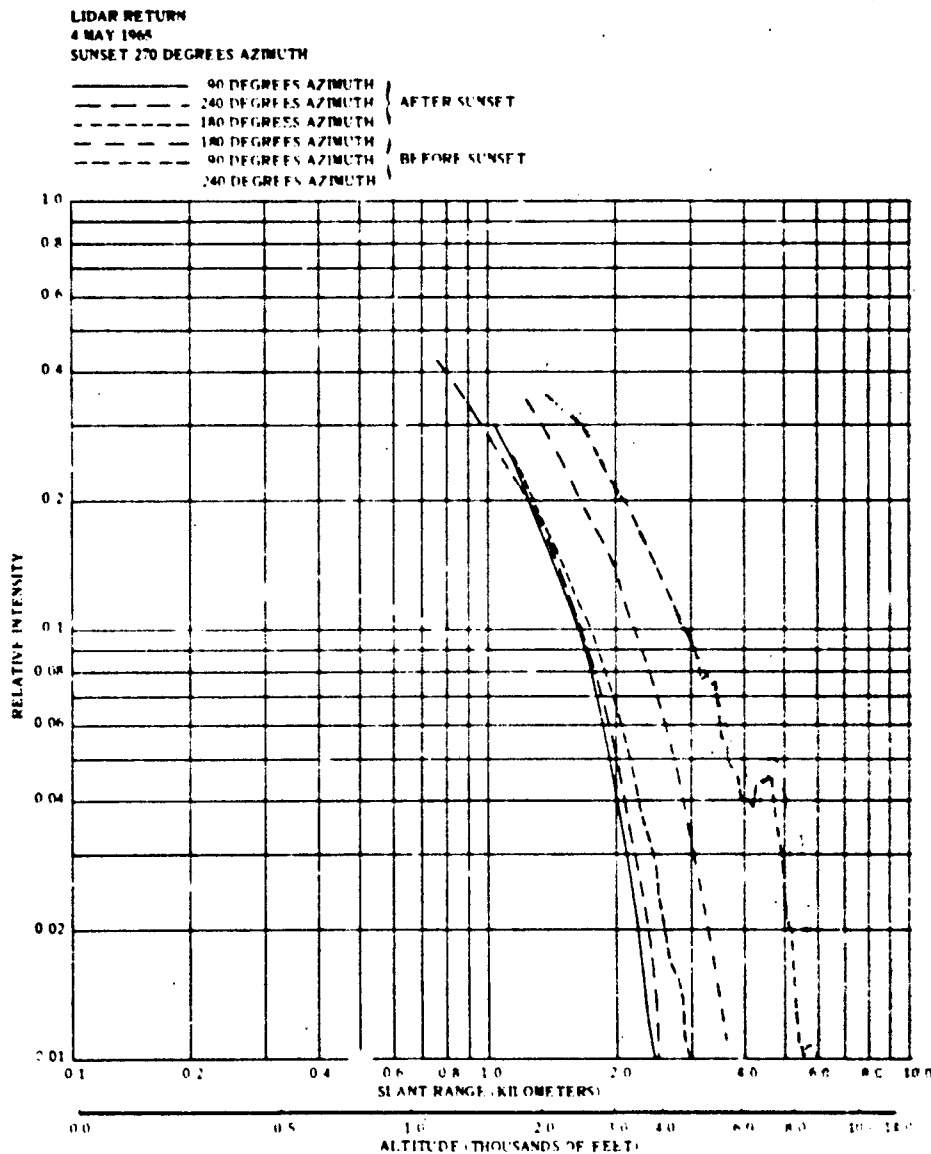


Figure 13. Solar Effects on LIDAR Return Before and After Sunset.

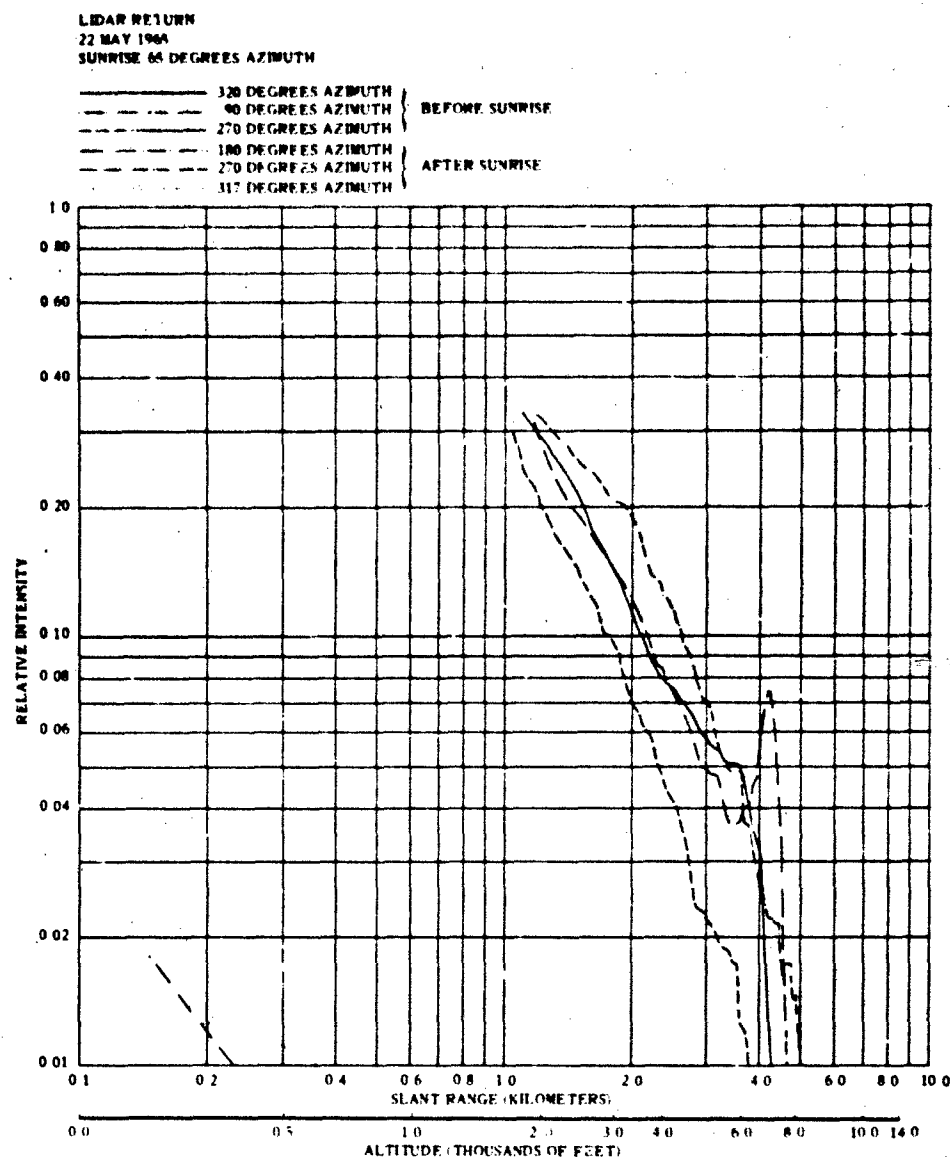


Figure 14. Solar Effects on LIDAR Return Before and After Sunrise.

Aircraft operations have a continuing requirement for slant visibility data for informing aircraft approaching for a landing. The present method used by the meteorologist for visibility reports is sometimes inaccurate and may only pertain to a certain quadrant or horizontal direction. The data now obtained with the LIDAR should contain information to compute slant visibility information. The difficulty is to reduce these data and to correlate the results. Using this visibility determination, there may result an approximation of the aerosol density which is the primary scattering agent in the LIDAR returns.

Continuing emphasis will be placed on stratus observation using the LIDAR for identifying those variables needed in predicting stratus formation and dissipation.

CONCLUSIONS

The LIDAR has demonstrated a great potential as a research and operational meteorological tool. When used in conjunction with meteorological information from other sources, the LIDAR data improves existing weather information. It is probable that the LIDAR will be capable of detecting and accurately measuring a wide variety of meteorological variables after engineering adaptations and improvements in techniques are accomplished. Some of these variables include measurements of wind speeds, temperature, water vapor, and atmospheric density. The LIDAR has been found useful for measuring the range to cloud bases and tops as well as stratus thickness. The existence and height of temperature inversions can be determined and concentrations of aerosols in apparently clear atmospheres can be detected. Immediate applications would include its use as a ceilometer aboard aircraft carriers as well as at air stations.

UNCLASSIFIED

Security Classification

DOCUMENT CONTROL DATA - R&D		
(Security classification of title, body of abstract and indexing annotation must be entered when the overall report is classified)		
1 ORIGINATING ACTIVITY (Corporate author) Pacific Missile Range Point Mugu, California		2a REPORT SECURITY CLASSIFICATION UNCLASSIFIED
		2b GROUP 1
3 REPORT TITLE DESCRIPTION AND APPLICATION OF LASER RADAR AT PACIFIC MISSILE RANGE		
4 DESCRIPTIVE NOTES (Type of report and inclusive dates)		
5 AUTHOR(S) (Last name, first name, initial) Karney, J. L.; Masterson, J.E.; and Hoehne, W. E.		
6 REPORT DATE 17 Aug 1966	7a TOTAL NO OF PAGES 19	7b NO OF REFS 1
8a CONTRACT OR GRANT NO. None	9a ORIGINATOR'S REPORT NUMBER(S) PMR-TM-66-6	
8b PROJECT NO.	9b OTHER REPORT NO(S) (Any other numbers that may be assigned this report)	
10 AVAILABILITY/LIMITATION NOTICES Distribution of this document is unlimited.		
11 SUPPLEMENTARY NOTES	12 SPONSORING MILITARY ACTIVITY Naval Air Systems Command	
13 ABSTRACT <p>A cooperative effort was undertaken by the Office of Naval Research, the Pacific Missile Range, and the Naval Air Systems Command to implement a proposed Stanford Research Institute program to design and fabricate a small laser radar to serve as a quasi-operational device for meteorological research. This prototype device, called the Mark III LIDAR (Light Detection and Ranging) was delivered to the Pacific Missile Range in February 1965 and is presently undergoing operational evaluation. A preliminary description of the data and results obtained are given.</p> <p>The LIDAR is a new and unique tool which promises to provide meteorologists and atmospheric physicists a means to accomplish tasks not possible using present equipment. The LIDAR can assist the meteorologist in making short-range forecasts by providing slant-range visibility data and quantitative measurements of stratus density and fog thickness.</p> <p>The LIDAR is capable of determining precise ranges to clouds (together with their bases and tops), measuring the height of temperature inversions, and detecting atmospheric phenomena in apparently clear atmospheres. At the present time, the LIDAR data are used in conjunction with observations from other sources to supplement and improve existing weather information. With relatively minor modifications, the LIDAR could significantly augment the present methods of gathering atmospheric data.</p>		

DD FORM 1473 1 JAN 64 0101-807-6800

UNCLASSIFIED

Security Classification

UNCLASSIFIED
Security Classification

14. KEY WORDS	LINK A		LINK B		LINK C	
	ROLE	WT	ROLE	WT	ROLE	WT
Laser radar Meteorological research Short-range forecasts Detecting atmospheric phenomena in apparently clear atmospheres Supplement and improve existing weather information Methods of gathering atmospheric data						

INSTRUCTIONS

1. **ORIGINATING ACTIVITY:** Enter the name and address of the contractor, subcontractor, grantee, Department of Defense activity or other organization (corporate author) issuing the report.
- 2a. **REPORT SECURITY CLASSIFICATION:** Enter the overall security classification of the report. Indicate whether "Restricted Data" is included. Marking is to be in accordance with appropriate security regulations.
- 2b. **GROUP:** Automatic downgrading is specified in DoD Directive 5200.10 and Armed Forces Industrial Manual. Enter the group number. Also, when applicable, show that optional markings have been used for Group 3 and Group 4 as authorized.
3. **REPORT TITLE:** Enter the complete report title in all capital letters. Titles in all cases should be unclassified. If a meaningful title cannot be selected without classification, show title classification in all capitals in parenthesis immediately following the title.
4. **DESCRIPTIVE NOTES:** If appropriate, enter the type of report, e.g., interim, progress, summary, annual, or final. Give the inclusive dates when a specific reporting period is covered.
5. **AUTHOR(S):** Enter the name(s) of author(s) as shown on or in the report. Enter last name, first name, middle initial. If military, show rank and branch of service. The name of the principal author is an absolute minimum requirement.
6. **REPORT DATE:** Enter the date of the report as day, month, year, or month, year. If more than one date appears on the report, use date of publication.
- 7a. **TOTAL NUMBER OF PAGES:** The total page count should follow normal pagination procedures, i.e., enter the number of pages containing information.
- 7b. **NUMBER OF REFERENCES:** Enter the total number of references cited in the report.
- 8a. **CONTRACT OR GRANT NUMBER:** If appropriate, enter the applicable number of the contract or grant under which the report was written.
- 8b, 8c, & 8d. **PROJECT NUMBER:** Enter the appropriate military department identification, such as project number, subproject number, system numbers, task number, etc.
- 9a. **ORIGINATOR'S REPORT NUMBER(S):** Enter the official report number by which the document will be identified and controlled by the originating activity. This number must be unique to this report.
- 9b. **OTHER REPORT NUMBER(S):** If the report has been assigned any other report numbers (either by the originator or by the sponsor), also enter this number(s).
10. **AVAILABILITY/LIMITATION NOTICES:** Enter any limitations on further dissemination of the report, other than those

imposed by security classification, using standard statements such as:

- (1) "Qualified requesters may obtain copies of this report from DDC."
- (2) "Foreign announcement and dissemination of this report by DDC is not authorized."
- (3) "U. S. Government agencies may obtain copies of this report directly from DDC. Other qualified DDC users shall request through _____."
- (4) "U. S. military agencies may obtain copies of this report directly from DDC. Other qualified users shall request through _____."
- (5) "All distribution of this report is controlled. Qualified DDC users shall request through _____."

If the report has been furnished to the Office of Technical Services, Department of Commerce, for sale to the public, indicate this fact and enter the price, if known.

11. **SUPPLEMENTARY NOTES:** Use for additional explanatory notes.

12. **SPONSORING MILITARY ACTIVITY:** Enter the name of the departmental project office or laboratory sponsoring (paying for) the research and development. Include address.

13. **ABSTRACT:** Enter an abstract giving a brief and factual summary of the document indicative of the report, even though it may also appear elsewhere in the body of the technical report. If additional space is required, a continuation sheet shall be attached.

It is highly desirable that the abstract of classified reports be unclassified. Each paragraph of the abstract shall end with an indication of the military security classification of the information in the paragraph, represented as (TS), (S), (C), or (U).

There is no limitation on the length of the abstract. However, the suggested length is from 150 to 225 words.

14. **KEY WORDS:** Key words are technically meaningful terms or short phrases that characterize a report and may be used as index entries for cataloging the report. Key words must be selected so that no security classification is required. Identifiers, such as equipment model designation, trade name, military project code name, geographic location, may be used as key words but will be followed by an indication of technical context. The assignment of links, roles, and weights is optional.

UNCLASSIFIED
Security Classification